中国激光

# 基于可饱和吸收体的700 mW单频2.05 μm线性腔铥钬共掺光纤激光器

蒋沛恒[1,2]，史朝督[1,2]，陈林[3]，付士杰[1,2]，盛泉[1,2*]，付彩玲[3**]，史伟[1,2***]，姚建铨[1,2]

[1]天津大学精密仪器与光电子工程学院，天津 300072；

[2]天津大学光电信息技术教育部重点实验室，天津 300072；

[3]深圳大学物理与光电工程学院光电子器件与系统教育部/广东省重点实验室，广东 深圳 518060

**摘要** 报道了基于掺铥光纤可饱和吸收体的单频2.05 μm线性腔铥钬共掺全光纤振荡器。腔内采用4.6 m长的铥钬共掺光纤作为增益介质，并利用未被泵浦的掺铥光纤作为可饱和吸收体实现选频，通过调整可饱和吸收体的长度可优化选频能力。在3.5 W的1570 nm激光泵浦下，获得了最高714 mW的2048.6 nm单频激光输出，相应的斜率效率为25.1%，激光光谱线宽为17 kHz。

**关键词** 激光器；单频光纤激光器；铥钬共掺光纤；可饱和吸收体；2 μm激光

**中图分类号** TN248 **文献标志码** A **DOI**：10.3788/CJL230873

## 1 引 言

2.0～2.2 μm波段单频激光光源[1-3]在生物医学、激光雷达、空间光通信等领域[4-6]中有广阔的应用前景。近年来，得益于高性能的掺铥光纤、掺钬光纤以及铥钬共掺光纤等增益光纤技术的发展[7-9]，该波段光纤激光光源得到了快速发展。虽然该波段光纤激光放大器的输出功率早已达到千瓦量级[10]，但是单频光纤激光振荡器的输出功率最高仅为百毫瓦量级。2021年，Walasik等[11]报道了基于掺铥石英光纤的分布反馈式(DFB)单频光纤振荡器，在800 mW的1567 nm激光泵浦下，获得了最高65 mW的2051 nm单频激光输出，由于DFB短腔中较短的有源光纤很难提供充足的增益，激光斜率效率仅为8.5%。在激光谐振腔中插入一段未被泵浦的掺杂光纤作为可饱和吸收体(SA)，当存在吸收带内波长的驻波场时，克尔效应对折射率的调制作用会在光纤中形成动态光栅，且可饱和吸收效应使得掺杂光纤在中心频率处的损耗很小，而在其他频率(纵模)处有较为明显的吸收损耗，因此能够实现类似窄带光栅的选频功能[12]。2022年，Zhang等[13]采用含有较长有源光纤的环形腔结构，以铥钬共掺光纤作为SA对掺铥光纤激光器进行选频，在2.02 W的1570 nm激光泵浦下，实现了掺铥光纤激光器最高215 mW的单频激光输出。由于信号光在环形腔中以行波形式传输，为了在SA光纤中形成驻波场实现选频功能，须额外引入环形器以及高反射光纤布拉格光栅(HR FBG)，故激光器的腔长达到21 m，相应的纵模间隔较小，这使得进一步增加泵浦功率时激光器无法保持单纵模运转状态。与环形腔相比，线性腔中的光场自身即为驻波，因此可在腔内直接插入SA实现选频功能，结构更为简单紧凑，较短的腔长也更有利于获得高功率单频激光。

相比于铥离子，钬离子的$^5I_7\rightarrow{}^5I_8$跃迁可以覆盖更长的激光波长，在2.0～2.2 μm区间有较大的发射截面，可以更高效地产生2 μm以上波段的激光[14]。但受限于掺钬光纤较低的增益系数，目前单频掺钬光纤激光器的输出功率最高仅为数十毫瓦。2009年，Wu等[15]首次报道了基于短腔分布布拉格反射(DBR)结构的单频掺钬光纤振荡器，利用长度为2 cm、掺杂钬离子的质量分数为3%的锗酸盐光纤作为增益介质，在500 mW的1950 nm掺铥光纤激光器泵浦下，获得了最高60 mW的2053 nm单频激光输出。2019年，Wolf等[16]报道了基于少模掺钬石英光纤的DFB单频光纤振荡器，在5.2 W的1125 nm掺镱光纤激光泵浦下，获得了最高52 mW的2070 nm单频激光输出。铥钬共掺光纤是另一种实现2 μm波段激光的有效增益介质，利用铥离子的$^3F_4$能级与钬离子的$^5I_7$能级之间的能量转换过程，可实现钬离子高效的$^5I_7\rightarrow{}^5I_8$跃迁，允许

**收稿日期**：2023-05-31；**修回日期**：2023-07-02；**录用日期**：2023-07-10；**网络首发日期**：2023-08-07

**基金项目**：国家自然科学基金(62105240，62275190，62075159，61975146)、山东省重点研发项目(2020CXGC010104，2021CXGC010202)、天津大学自主创新基金(2023XPD-0020)

**通信作者**：*shengquan@tju.edu.cn；**fucailing@szu.edu.cn；***shiwei@tju.edu.cn

使用相对较为成熟的 793 nm 或 1570 nm 泵浦源获得高功率 2 μm 波段激光输出[17-19]。

本文利用铥钬共掺光纤搭建了线性腔激光振荡器，结合掺铥光纤作为可饱和吸收体的选频功能，实现了高功率 2.05 μm 单频激光运转。在 3.5 W 的 1570 nm 激光泵浦下，获得了 714 mW 的单频激光输出。在实验中分析了不同长度可饱和吸收体对激光效率及纵模特性的影响，相关结果为高功率单频铥钬共掺光纤激光器以及线性腔 SA 选频单频光纤激光器的参数优化提供了参考。

## 2 实验装置

线性腔单频铥钬共掺光纤振荡器的结构如图 1 所示。振荡器中增益光纤选用长度为 4.6 m 的单模铥钬共掺光纤，纤芯/包层尺寸分别为 9 μm/125 μm，光纤在 1570 nm 处的纤芯吸收系数为 43 dB/m。泵浦源为单模 1570 nm 光纤激光器，最高输出功率为 3.5 W。激光器采用正向泵浦方式，泵浦光经过一个 1570 nm/2000 nm 滤波型波分复用器 1（FWDM1）耦合进增益光纤，另一 FWDM2 置于增益光纤末端，用于滤除剩余泵浦光。一对光纤布拉格光栅置于振荡器两端构成谐振腔，输出端的部分反射光纤布拉格光栅（PR FBG）的中心波长为 2048.69 nm，反射率为 39.7%，3 dB 带宽为 0.075 nm，尾纤进行 8°角斜切。HR FBG 的中心波长为 2048.76 nm，反射率＞99.5%，3 dB 带宽为 0.35 nm。为实现激光器的单纵模运转，在 HR FBG 和 FWDM1 之间加入了一段未泵浦的掺铥光纤作为 SA，其在 2.05 μm 处的吸收系数约为 0.5 dB/m。虽然铥钬共掺光纤中的钬离子在 2.05 μm 附近有更大的吸收截面，更有利于形成 SA 内的动态光栅，但是高吸收系数的 SA 会影响激光器的效率，无法应用较长的光纤增强选频功能[20-21]。因此，本实验采用了 2 μm 波段吸收截面相对较小的掺铥光纤作为 SA，通过对其长度进行优化，在增强选频功能的同时获得了高功率单频激光。

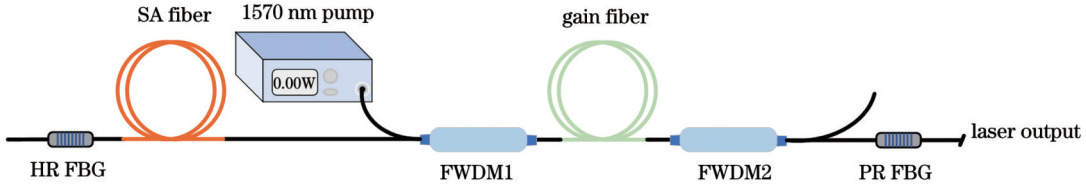


图 1 单频铥钬共掺光纤激光器的结构示意图

Fig. 1 Structural diagram of single-frequency $Tm^{3+}$/$Ho^{3+}$-codoped fiber laser

## 3 结果与分析

根据此前的研究结果可知，对于掺杂浓度相同的 SA 光纤，其长度越长，形成的动态光栅的带宽越窄，越有利于实现单纵模运转[13,22]。但过长的 SA 光纤会使信号光产生损耗，影响激光器效率，因此在实验中需要优化 SA 光纤长度，平衡选频能力和损耗，从而获得高功率单频激光。实验中分别研究了未加入 SA 以及 SA 长度为 1.5 m 和 2.5 m 时激光器的输出特性。采用功率计测量得到的激光输出功率曲线如图 2 所示，其中离散点为实验测量数据，实线为线性拟合结果，实心/空心标记分别表示该功率下的单纵模/多纵模运转。未加入 SA 时，激光阈值为 0.53 W，激光输出功率随泵浦功率线性增长；当泵浦功率为 3.5 W 时，获得的最大激光输出功率为 813 mW，激光斜率效率（$\eta_s$）为 26.9%，光光效率为 23.2%。受限于 FWDM1 的功率承受能力，实验中没有继续增加泵浦功率。在最大输出功率下，通过 FWDM2 的反射端口测得的剩余泵浦功率仅为 10 mW，表明 4.6 m 长的铥钬共掺光纤实现了充分的泵浦吸收。当腔内分别加入长度为 1.5 m 和 2.5 m 的 SA 时，激光阈值分别上升到 0.62 W 和 0.72 W，最大泵浦功率 3.5 W 下的激光输出功率分别降至 773 mW 和 714 mW，对应的斜率效率分别为 26.1% 和 25.1%，光光效率为 22.1% 和 20.4%。由于作为 SA 的

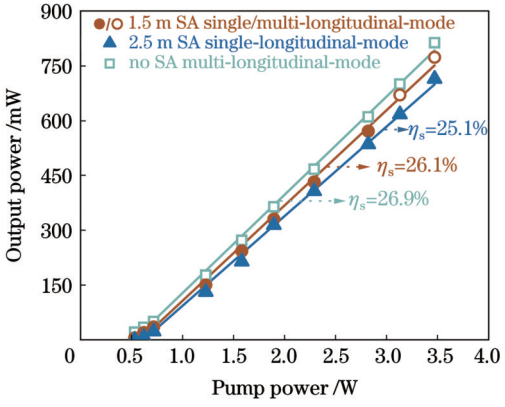


图 2 铥钬共掺光纤激光器输出功率随泵浦功率的增长曲线（点为实验测量数据，实线为线性拟合结果）

Fig. 2 Output power of $Tm^{3+}$/$Ho^{3+}$-codoped fiber laser versus pump power with experimental measurement data shown by points and linear fitting results shown by solid lines

掺铥光纤对信号光存在吸收，SA 长度的增加会在一定程度上降低激光器的效率。

在不同长度 SA 条件下，输出激光的纵模特性表现出明显差异。我们采用法布里-珀罗扫描干涉仪（FPI，分辨率为 67 MHz）和频谱分析仪测量了不同长度 SA 下激光器的纵模特性。由图 2 可以看出：在未加入 SA 时，激光器始终处于多纵模运转状态；当 SA 长度为 1.5 m 时，SA 的引入使激光器的纵模特性

得到优化，在 2.8 W 及以下的泵浦功率范围内激光器保持单纵模运转，进一步增加泵浦功率，激光器则变为多纵模运转状态，最高单纵模输出功率为 571 mW；而当 SA 长度为 2.5 m 时，激光器能够始终保持稳定的单纵模运转状态，3.5 W 最大泵浦功率下单纵模输出功率可达到 714 mW。图 3(a)、(b)分别给出了上述两种 SA 长度下输出功率均为 714 mW 时的激光频谱和纵模特性，其中 FSR 为自由光谱范围。当 SA 长度为 1.5 m 时，FPI 扫描波形显示激光器为多纵模运转状态，在频谱中可观察到呈周期性分布的频率峰，频率间隔为 12 MHz，与此时激光谐振腔(腔长 8.6 m)的自由光谱范围吻合，因此此频率峰的产生是相邻纵模拍频引起的。而当 SA 的长度增加至 2.5 m 时，FPI 扫描波形显示激光器为稳定的单纵模运转状态，在激光频谱中未观察到相邻纵模间的拍频峰。由前述 SA 实现选频功能的原理可知，当 SA 长度为 1.5 m 时，其选频能力不足以在高泵浦功率下支撑激光器的单纵模运转状态。而随着 SA 的长度增加到 2.5 m，选频能力加强，实现了稳定的单纵模激光输出。

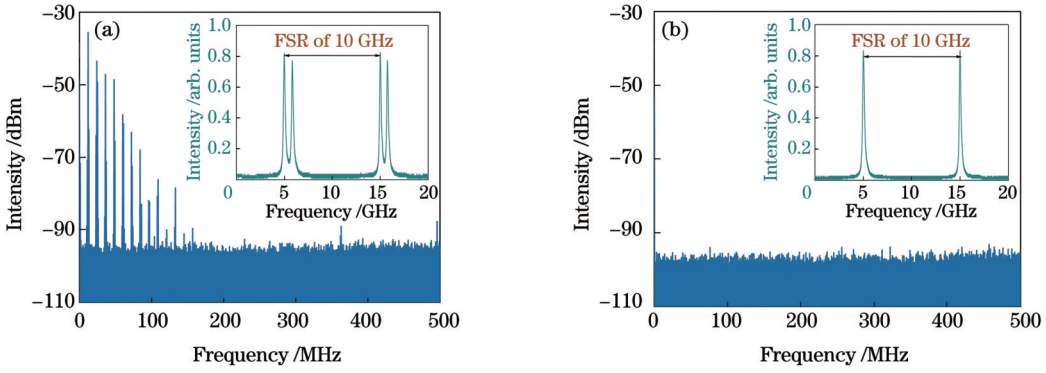


图 3 不同 SA 长度下输出功率为 714 mW 时铥钬共掺光纤激光器的频谱和波形。(a) 1.5 m；(b) 2.5 m

Fig. 3 Spectra and waveforms of $Tm^{3+}$/$Ho^{3+}$-codoped fiber laser at output power of 714 mW under different SA lengths. (a) 1.5 m; (b) 2.5 m

在单频激光最大输出功率为 714 mW 的条件下，光谱分析仪(OSA，分辨率为 0.05 nm)记录的激光光谱如图 4 所示。激光中心波长为 2048.6 nm，在 1.9～2.0 μm 波段存在一定的放大自发辐射(ASE)成分，其中在 1950 nm 和 2000 nm 附近存在两个峰，分别对应 $Tm^{3+}$ 的 $^3F_4 \rightarrow {}^3H_6$ 跃迁和 $Ho^{3+}$ 的 $^5I_7 \rightarrow {}^5I_8$ 跃迁，激光输出相对 ASE 的信噪比为～60 dB。图 4 插图为单频激光输出功率为 714 mW 时 2047～2050 nm 范围内的激光光谱，输出激光相对带内 ASE 的信噪比在 75 dB 以上。

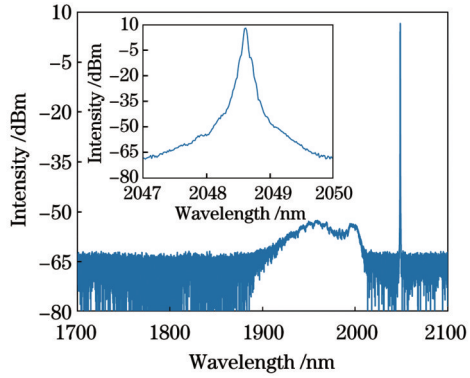


图 4 单频激光输出功率为 714 mW 时的激光光谱

Fig. 4 Laser spectrum when output power of single-frequency laser is 714 mW

实验中利用光电探测器(PD)和频谱分析仪测量了激光器的相对强度噪声(RIN)特性。图 5(a)、(b)所示分别为激光输出功率为 407 mW 和 714 mW 时的 RIN 特性，激光器的弛豫振荡频率从 0.17 MHz 移动到 0.20 MHz，弛豫振荡峰值强度由 −102 dB/Hz 增加至 −100 dB/Hz。在 1 MHz 以上频率范围内 RIN 接近测试系统 −147 dB/Hz 的噪声极限。图 5 中 0.4 MHz 附近的频率峰在没有光信号注入的条件下依然存在，推断是测量系统中的电噪声。

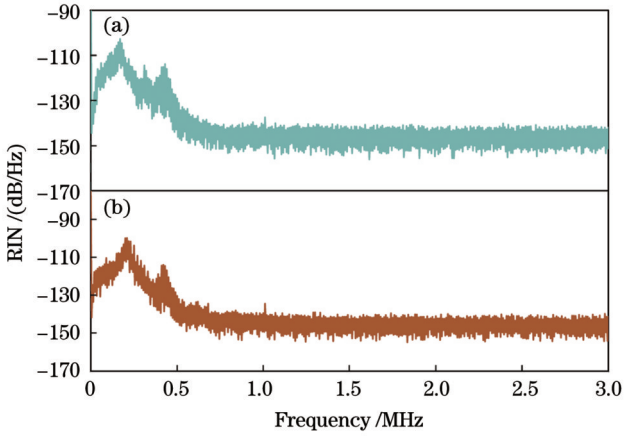


图 5 2050 nm 单频光纤激光器在不同输出功率下的相对强度噪声。(a) 407 mW；(b) 714 mW

Fig. 5 RIN of 2050 nm single-frequency fiber laser under different output powers. (a) 407 mW; (b) 714 mW

采用延迟自外差系统和频谱分析仪在 714 mW 最高输出功率下测量单频激光光谱线宽，结果如图 6 所

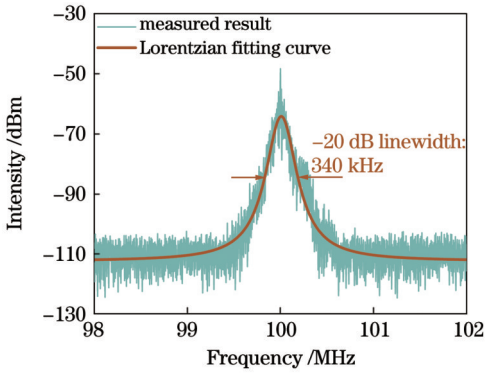


图 6 最高单频输出功率为 714 mW 时延迟自外差系统测得的 2050 nm 单频光纤激光的线宽

Fig. 6 Measured linewidth of 2050 nm single-frequency fiber laser using delayed self-heterodyne system at maximum single-frequency output power of 714 mW

示。考虑到石英光纤在 2.05 μm 处的传输损耗，测量中的延迟光纤采用了 100 m 长的单模光纤。测量得到的拍频信号功率谱呈洛伦兹线型，在主峰两翼未观察到周期性分布的相干包络，因此洛伦兹线型包络的宽度可以作为待测激光器线宽的一个参考[23-25]，经洛伦兹拟合后得到其−20 dB 线宽为 340 kHz，相应激光线宽为 17 kHz，更准确的线宽信息可通过待测激光与频率相近且线宽较窄的单频激光的拍频获得。

## 4 结 论

报道了基于掺铥光纤 SA 的线性腔 2048.6 nm 单频铥钬共掺光纤激光器。实验研究了 SA 长度对激光输出功率及纵模特性的影响，在 SA 长度为 2.5 m 的条件下，获得了最高 714 mW 的单频激光功率，对应的激光斜率效率为 25.1%，光光效率为 20.4%。在最大输出功率条件下，激光的信噪比达到 60 dB，相对强度噪声峰值为−102 dB/Hz，激光线宽为 17 kHz。该结果证明了基于 SA 光纤选频的线性腔结构可实现高功率单频激光运转，为单频激光振荡器输出功率的优化提供了参考。

## 参 考 文 献


[1] Fu S J, Shi W, Feng Y, et al. Review of recent progress on single-frequency fiber lasers[J]. Journal of the Optical Society of America B, 2017, 34(3): A49-A62.

[2] Fu S J, Shi G N, Sheng Q, et al. Dual-wavelength fiber laser above 2 μm based on cascaded single mode-multimode-single mode structures[J]. Optics Express, 2016, 24(11): 11282-11289.

[3] 史伟, 付士杰, 盛泉, 等. 高性能单频光纤激光器研究进展：2017—2021(特邀)[J]. 红外与激光工程, 2022, 51(1): 20210905.
Shi W, Fu S J, Sheng Q, et al. Research progress on high-performance single-frequency fiber lasers: 2017-2021 (Invited)[J]. Infrared and Laser Engineering, 2022, 51(1): 20210905.

[4] Renz G, Bohn W. Two-micron thulium-pumped-holmium laser source for DIRCM applications[J]. Proceedings of SPIE, 2007, 6552: 655202.

[5] Barria J B, Mammez D, Cadiou E, et al. Multispecies high-energy emitter for $CO_2$, $CH_4$, and $H_2O$ monitoring in the 2 μm range[J]. Optics Letters, 2014, 39(23): 6719-6722.

[6] Szlauer R, Götschl R, Razmaria A, et al. Endoscopic vaporesection of the prostate using the continuous-wave 2- μm thulium laser: outcome and demonstration of the surgical technique [J]. European Urology, 2009, 55(2): 368-375.

[7] Shi C D, Fu S J, Shi G N, et al. All-fiberized single-frequency silica fiber laser operating above 2 μm based on SMS fiber devices [J]. Optik, 2019, 187: 291-296.

[8] Tench R E, Romano C, Williams G M, et al. Two-stage performance of polarization-maintaining holmium-doped fiber amplifiers[J]. Journal of Lightwave Technology, 2019, 37(4): 1434-1439.

[9] Beaumont B, Bourdon P, Barnini A, et al. High efficiency holmium-doped triple-clad fiber laser at 2120 nm[J]. Journal of Lightwave Technology, 2022, 40(19): 6480-6485.

[10] Thomas E, Ryan L, Imtiaz M, et al. 1-kW, all-glass Tm: fiber laser[EB/OL]. [2023-05-06]. http://www.qpeak.com/sites/psicorp.com/files/articles/PW%202010%201kW%20Tm_fiber%20laser.pdf.

[11] Walasik W, Traoré D, Amavigan A, et al. 2 μm narrow linewidth all-fiber DFB fiber Bragg grating lasers for Ho- and Tm-doped fiber-amplifier applications[J]. Journal of Lightwave Technology, 2021, 39(15): 5096-5102.

[12] Zhang J X, Sheng Q, Zhang L, et al. 2.56 W single-frequency all-fiber oscillator at 1720 nm[J]. Advanced Photonics Research, 2022, 3(2): 2100256.

[13] Zhang L, Sheng Q, Chen L, et al. Single-frequency Tm-doped fiber laser with 215 mW at 2.05 μm based on a Tm/Ho-codoped fiber saturable absorber[J]. Optics Letters, 2022, 47(15): 3964-3967.

[14] Kuan P W, Fan X K, Li X A, et al. High-power 2.04 μm laser in an ultra-compact Ho-doped lead germanate fiber[J]. Optics Letters, 2016, 41(13): 2899-2902.

[15] Wu J F, Yao Z D, Zong J E, et al. Single frequency fiber laser at 2.05 μm based on Ho-doped germanate glass fiber[J]. Proceedings of SPIE, 2009, 7395: 71951K.

[16] Wolf A A, Skvortsov M I, Kamynin V A, et al. All-fiber holmium distributed feedback laser at 2.07 μm[J]. Optics Letters, 2019, 44(15): 3781-3784.

[17] Oh K, Morse T F, Weber P M, et al. Continuous-wave oscillation of thulium-sensitized holmium-doped silica fiber laser[J]. Optics Letters, 1994, 19(4): 278-280.

[18] Wang Z H, Zhang B, Liu J, et al. Recent developments in mid-infrared fiber lasers: status and challenges[J]. Optics & Laser Technology, 2020, 132: 106497.

[19] Xue G H, Zhang B, Yin K, et al. Ultra-wideband all-fiber tunable Tm/Ho-co-doped laser at 2 μm[J]. Optics Express, 2014, 22(21): 25976-25983.

[20] Kishi N, Yazaki T. Frequency control of a single-frequency fiber laser by cooperatively induced spatial-hole burning[J]. IEEE Photonics Technology Letters, 1999, 11(2): 182-184.

[21] Poozesh R, Madanipour K, Parvin P. High SNR watt-level single frequency Yb-doped fiber laser based on a saturable absorber filter in a cladding-pumped ring cavity[J]. Journal of Lightwave Technology, 2018, 36(20): 4880-4886.

[22] Zhang J X, Sheng Q A, Zhang L, et al. Single-frequency 1.7-μm Tm-doped fiber laser with optical bistability of both power and longitudinal mode behavior[J]. Optics Express, 2021, 29(14): 21409-21417.

[23] Zhu N H, Man J W, Zhang H G, et al. Lineshape analysis of the beat signal between optical carrier and delayed sidebands[J]. IEEE Journal of Quantum Electronics, 2010, 46(3): 347-353.

[24] Yang C S, Zhao Q L, Feng Z M, et al. 1120 nm kHz-linewidth single-polarization single-frequency Yb-doped phosphate fiber laser [J]. Optics Express, 2016, 24(26): 29794-29799.

[25] Yang C S, Guan X C, Lin W, et al. Efficient 1.6 μm linearly-polarized single-frequency phosphate glass fiber laser[J]. Optics Express, 2017, 25(23): 29078-29085.

# 700 mW Single-Frequency Linear Cavity $Tm^{3+}/Ho^{3+}$-Codoped Fiber Laser at 2.05 μm Based on Saturable Absorber

Jiang Peiheng[1,2], Shi Chaodu[1,2], Chen Lin[3], Fu Shijie[1,2], Sheng Quan[1,2*], Fu Cailing[3**], Shi Wei[1,2***], Yao Jianquan[1,2]

[1]*School of Precision Instrument and Optoelectronics Engineering, Tianjin University, Tianjin* 300072, *China*;

[2]*Key Laboratory of Optoelectronics Information Technology, Ministry of Education, Tianjin University, Tianjin* 300072, *China*;

[3]*Key Laboratory of Optoelectronic Devices and Systems of Ministry of Education and Guangdong Province, College of Physics and Optoelectronics Engineering, Shenzhen University, Shenzhen* 518060, *Guangdong, China*

## Abstract

**Objective** Single-frequency lasers with wavelengths above 2 μm have attracted significant interest because of their numerous applications in areas such as biomedicine, Doppler LiDAR, and space optical communication. Although the power of the fiber master oscillator power amplifier (MOPA) around 2 μm has already reached the kilowatt level, the output powers of single-longitudinal-mode (SLM) laser oscillators in this wavelength region are still limited to the hundred-milliwatt level due to the laser gain and frequency-selection approaches. When a piece of unpumped rear-earth doped fiber is found inside the cavity of a laser, the standing wave field inside it results in a dynamic grating because of the Kerr effect. Moreover, the absorption loss of the doped fiber is small under the oscillating longitudinal mode but considerably larger under the side modes. These processes may provide a strong frequency-selection effect, thus allow lasers with longer cavity lengths and resulting higher laser gain to operate in SLM. In this study, we demonstrate an efficient SLM fiber laser at 2050 nm. A piece of $Tm^{3+}/Ho^{3+}$-codoped fiber is used as gain fiber to provide a laser gain at over 2 μm wavelength, while a piece of $Tm^{3+}$-doped fiber is inserted into the laser cavity as the saturable absorber (SA) for frequency selection. A linear cavity scheme is adopted, rather than the ring cavity usually used in SLM cavity lasers, based on the fiber SA approach to enhance longitudinal mode spacing for a higher power SLM output. A maximum SLM 2050-nm laser output power of 714 mW is obtained under the incident 1570-nm pump power of 3.5 W.

**Methods** A schematic of the SLM laser is given in Fig. 1. The gain fiber used is a piece of 9-μm/125-μm $Tm^{3+}/Ho^{3+}$-codoped fiber with a length of 4.6 m. The pump light launched from a 1570-nm fiber laser is coupled into the core of the active fiber via the filter wavelength division multiplexer 1 (FWDM1). Two fiber Bragg gratings (FBGs) are used to make the linear laser cavity. The reflectivity and 3-dB bandwidth of the partially-reflective FBG with its pigtail angle cleaved at 8° are 39.7% and 0.075 nm, respectively. The $Tm^{3+}$-doped SA fiber used has a core absorption coefficient of 0.5 dB/m at 2050 nm. Another FWDM2 is used to couple the residual pump out of the oscillator.

**Results and Discussions** It is known that longer SA fibers have a stronger frequency-selection capability; however, their oscillation mode losses are greater, resulting in reduced laser power and efficiency. In the experiment, we use SA fibers with lengths of 1.5 m and 2.5 m. The laser wavelength determined by the FBGs is 2048.6 nm. Without the SA fiber in the cavity, the laser output power is 813 mW under the maximum 1570-nm pump power of 3.5 W, with a slope efficiency of 26.9%. When the 1.5-m and 2.5-m long SA fibers are added to the cavity, the laser output power under the same pump power decreases to 773 mW and 714 mW, with slope efficiencies of 26.1% and 25.1%, respectively, as shown in Fig. 2. The laser threshold also increases from 0.53 W without the SA to 0.62 W and 0.72 W when the two pieces of SA are used. With the 1.5-m long SA fiber, the laser is in SLM with a pump power of 2.8 W and lower (571-mW output power), which is confirmed using a scanning Fabry-Perot interferometer and the spectrum. For higher pump powers, the laser becomes multi-longitudinal-mode because of the insufficient frequency-selection capability. When the 2.5-m long SA fiber is used, the laser maintains stable SLM operation from the 0.72-W threshold pump power to the 3.5-W maximum pump power, with a maximum output power of 714 mW [Fig. 3(b)]. The optical spectrum recorded by the optical spectrum analyzer shows an optical signal-to-noise ratio (OSNR) of ~60 dB between the 2048.6-nm laser and the 1.9–2.0 μm amplifier spontaneous emission (ASE) peak, whereas the in-band OSNR is beyond 75 dB (Fig. 4). The 3-dB spectral linewidth of the SLM output is measured to be 17 kHz using the delayed self-heterodyne interferometer technique at the maximum power of 714 mW (Fig. 6).

**Conclusions** In this study, we demonstrate a linear cavity SLM $Tm^{3+}/Ho^{3+}$-codoped fiber based on a $Tm^{3+}$-doped SA fiber for frequency selection. The laser delivers a 714-mW SLM output at 2048.6 nm under a maximum 1570-nm pump power of 3.5 W, with a slope efficiency of 25.1% and an optical efficiency of 20.4%. The influence of the SA fiber length on the frequency-selection capability and the supported SLM output power is experimentally investigated. The results show that a linear cavity with an SA fiber inside can achieve a high-power SLM laser output.

**Key words** lasers; single-frequency fiber lasers; $Tm^{3+}/Ho^{3+}$-codoped fiber; saturable absorber; 2 μm laser